Author Manuscript

Author Manuscript

Author Manuscript

Author Manuscript

HHS Public Access

Author manuscript

J Biomech. Author manuscript; available in PMC 2017 May 03.

Published in final edited form as:

J Biomech. 2016 May 3; 49(7): 1078–1084. doi:10.1016/j.jbiomech.2016.02.038.

EFFECTS OF FOLLOWER LOAD AND RIB CAGE ON INTERVERTEBRAL DISC PRESSURE AND SAGITTAL PLANE CURVATURE IN STATIC TESTS OF CADAVERIC THORACIC SPINES

Dennis E. Anderson[1,2], **Erin M. Mannen**[4], **Hadley L. Sis**[3], **Benjamin M. Wong**[3], **Eileen S. Cadel**[3], **Elizabeth A. Friis**[3,4], and **Mary L. Bouxsein**[1,2]

[1]Center for Advanced Orthopaedic Studies, Beth Israel Deaconess Medical Center, Boston, USA

[2]Department of Orthopedic Surgery, Harvard Medical School, Boston, MA, USA

[3]Bioengineering Graduate Program, The University of Kansas, Lawrence, KS, USA

[4]Department of Mechanical Engineering, The University of Kansas, Lawrence, KS, USA

Abstract

The clinical relevance of mechanical testing studies of cadaveric human thoracic spines could be enhanced by using follower preload techniques, by including the intact rib cage, and by measuring thoracic intervertebral disc pressures, but studies to date have not incorporated all of these components simultaneously. Thus, this study aimed to implement a follower preload in the thoracic spine with intact rib cage, and examine the effects of follower load, rib cage stiffening and rib cage removal on intervertebral disc pressures and sagittal plane curvatures in unconstrained static conditions. Intervertebral disc pressures increased linearly with follower load magnitude. The effect of the rib cage on disc pressures in static conditions remains unclear because testing order likely confounded the results. Disc pressures compared well with previous reports *in vitro*, and comparison with *in vivo* values suggests the use of a follower load of about 400 N to approximate loading in upright standing. Follower load had no effect on sagittal plane spine curvature overall, suggesting successful application of the technique, although increased flexion in the upper spine and reduced flexion in the lower spine suggest that the follower load path was not optimized. Rib cage stiffening and removal both increased overall spine flexion slightly, although with differing effects at specific spinal locations. Overall, the approaches demonstrated here will support the use of follower preloads, intact rib cage, and disc pressure measurements to enhance the clinical relevance of future studies of the thoracic spine.

Please address all correspondence to: Dennis Anderson, Beth Israel Deaconess Medical Center, 330 Brookline Ave, RN115, Boston, MA 02215, Phone: 617-667-5380, Fax: 617-667-7175, danders7@bidmc.harvard.edu.

Conflict of Interest Statement

The authors state that they have no conflict of interest to disclose.

Publisher's Disclaimer: This is a PDF file of an unedited manuscript that has been accepted for publication. As a service to our customers we are providing this early version of the manuscript. The manuscript will undergo copyediting, typesetting, and review of the resulting proof before it is published in its final citable form. Please note that during the production process errors may be discovered which could affect the content, and all legal disclaimers that apply to the journal pertain.

Author Manuscript Author Manuscript Author Manuscript Author Manuscript

Keywords

Thoracic spine; Mechanical Testing; Follower load; Rib cage; Intervertebral Disc Pressure

1. Introduction

Better understanding of thoracic spine biomechanics is needed to improve treatments for common clinical conditions affecting the thoracic spine, which include scoliosis (Asher and Burton, 2006), hyperkyphosis (Kado et al., 2007), vertebral fractures (Van der Klift et al., 2002), and thoracic spinal pain (Briggs et al., 2009). The presence of the rib cage is a distinguishing feature of the thoracic spine, and mechanical testing studies indicate that the rib cage adds significantly to overall thoracic stiffness, (Brasiliense et al., 2011; Mannen et al., 2015b; Watkins et al., 2005). In addition, some treatments for thoracic and spinal deformity utilize implants that attach to the ribs (Campbell, 2013), making the interaction between thoracic spine and rib cage of direct clinical importance in these situations. Furthermore, age-related increases in costal cartilage calcification (Teale et al., 1989) or sternocostal joint osteophytes (Schils et al., 1989) could act to locally stiffen the rib cage, altering the interaction between spine and rib cage. Thus, studies of thoracic spine biomechanics should include the rib cage to enhance anatomical and clinical relevance.

Because of the importance of the rib cage, several recent studies examining basic and clinical biomechanics in the human cadaveric thoracic spine have left the rib cage intact during testing (Healy et al., 2015; Mannen et al., 2015a; Perry et al., 2014). However, these studies did not include a physiological level of spinal compressive loading. A follower preload technique increases the compressive load that a cadaveric spine specimen can carry (Patwardhan et al., 1999), allowing physiologically realistic levels of loading during mechanical testing studies. A few studies including the thoracic spine have implemented a follower load technique (Auerbach et al., 2012; Buttermann and Beaubien, 2008; Stanley et al., 2004), but these studies were performed without the rib cage intact. Because including both rib cage and follower load would increase the clinical relevance of biomechanical testing in cadaveric thoracic spines, there is a need to develop methods to incorporate both into mechanical testing protocols.

While the loading of a particular vertebral level within an intact spine cannot be measured directly, pressure within intervertebral discs is known to correlate strongly with directly applied compressive loading in cadaveric tests (Nachemson, 1960; Pollintine et al., 2004). Disc pressures have frequently been measured in cadaveric tests of lumbar spine segments (Dolan et al., 2013; Nachemson, 1960; Pollintine et al., 2004), and less often in thoracic specimens (Dolan et al., 2013). Several studies have measured lumbar disc pressures while applying follower loads to lumbar or thoracolumbar spine specimens (Auerbach et al., 2012; Buttermann and Beaubien, 2008; Rohlmann et al., 2001; Wilke et al., 2003). Disc pressure measurements have been also used in *in vivo* experiments as indicators of both lumbar (Nachemson and Morris, 1964; Sato et al., 1999; Schultz et al., 1982; Wilke et al., 2001) and thoracic (Polga et al., 2004) spinal loading. Thus, thoracic disc pressures may prove to be

Author Manuscript Author Manuscript Author Manuscript Author Manuscript

useful measurements in tests of cadaveric thoracic spines, but these have not been previously measured under follower load or with the rib cage intact.

As follower load implementation within the confines of an intact rib cage requires adaptation of previous approaches, the purpose of this study was to determine the effects of follower load and rib cage conditions on intervertebral disc pressures and sagittal plane curvature in static, upright, unconstrained loading conditions, providing a baseline to support future studies using these techniques. We hypothesized that disc pressure would increase with increasing follower load, would decrease by artificially stiffening the rib cage, and would increase by the removal of the rib cage from the spine. We also assessed differences in disc pressure between two vertebral levels (T4-T5 vs T8-T9). We also hypothesized that spine curvature would vary between rib cage conditions, but not with follower load, when examined overall, regionally, or at specific levels.

2. Methods

2.1 Specimens

Eight fresh-frozen full human cadaveric thoracic spines (T1-T12) with the rib cage intact (4 female and 4 male, mean age 67 years, range 61–71) were obtained from an anatomic tissue bank. Specimens had no reported history of moderate-severe vertebral fracture, severe scoliosis or kyphosis, or spinal surgery. Muscles and soft tissues were removed, except the intercostal muscles which were left intact. Several rib fractures were fixed by plating in one specimen prior to testing, which has been done previously in mechanical testing of cadaveric full thoracic spines with rib cage (Watkins et al., 2005). The ends of each specimen (T1 and T12) were potted in auto-body filler (Bondo, 3M, St. Paul, MN, USA) parallel to their vertebral end plates.

2.2 Follower load application

The follower load approach of previous studies (Patwardhan et al., 1999; Stanley et al., 2004) was adapted to insert the follower load hardware within the confines of the intact rib cage. In this study a fully threaded rod was inserted laterally through vertebral bodies at levels T3 – T11. Steel cable was attached to the potting at T1 and fed through a series of rod ends with ball joints attached to the ends of the threaded rods on each side of the spine (Figure 1). The potting at the inferior end of each specimen (T12) was bolted to a horizontal surface for testing. Below T11, the cables were fed through pulleys positioned to continue the curvature of the follower load cable. To apply a follower load, weights equaling half of the total load were hung from the end of each cable.

2.3 Testing Conditions

Testing was performed on fully thawed specimens at room temperature, and specimens were frequently sprayed with saline solution to help maintain hydration. Measurements were performed under three testing conditions, first with normal intact rib cage, then with an artificially stiffened rib cage, and finally with the entire rib cage removed by cutting the ribs just lateral to the costotransverse joints as done in prior studies (Mannen et al., 2015b; Watkins et al., 2005) (Figure 2). The stiffened rib cage condition used metal plates to bridge

Author Manuscript Author Manuscript Author Manuscript Author Manuscript

the costal cartilage and sternocostal joints bilaterally for ribs 2–5, with the goal of simulating potential effects of cartilage calcification or sternocostal joint osteophytes by reducing motion across these connections. Within each testing condition, four follower load levels were applied: 0 N, 200 N, 400 N, and 600 N.

2.4 Measurements

Disc pressures were measured using pressure transducers side mounted on 1.3 mm diameter needles (Gaeltec, Isle of Skye, Scotland) inserted in the T4-T5 and the T8-T9 discs (Figure 1). The pressure transducers were positioned to record pressure in the center of the nucleus pulposus, with locations confirmed by radiography. Disc pressures were recorded at 10 Hz, and an average value taken to represent the static pressure under each testing condition.

Motion-capture pins (Optotrak, Northern Digital Inc., Waterloo, ON, Canada) were inserted into the potting material at T1, and the left pedicles of T2, T4, T5, T8, T9 and T11, and vertebral position and orientation were recorded under each test condition. Local coordinate systems were developed (Wilke et al., 1998), and segmental sagittal curvatures were found overall (T1-T12), regionally (T1-T4, T4-T8, T8-T12) and at specific individual levels (T1-T2, T4-T5, T8-T9, T11-T12).

2.5 Statistical Analysis

The effects of follower load and rib cage condition (Intact, Stiffened, No Ribs) on disc pressure and spine sagittal curvature were examined with mixed effects regression models, including follower load magnitude as a continuous fixed effect, rib cage condition as a categorical fixed effect with Intact as the baseline condition, and adjusting for specimen as a random variable to account for potential variation between specimens. A separate model was constructed for each disc pressure measured (T4-T5 and T8-T9), as well as for overall curvature (T1-T12), regional curvatures (T1-T4, T4-T8 and T8-T12), and individual curvatures (T1-T2, T4-T5, T8-T9 and T11-T12). Linear combinations of coefficients from the primary regression were used to estimate the intercept (outcome at 0 follower load) and slope (change with follower load) for Stiffened and No Ribs conditions, and significance of slope and differences of slope and intercept from Intact condition were examined. Useful pressure measures were not obtained in a few discs (recorded pressure remained at or near 0), and these were excluded from analyses. The difference in pressure between levels (T4-T5 vs. T8-T9) was also examined for effects of load and testing condition. Significance was set at $a = 0.05$, and analyses were performed in Stata/IC 13.1 (StataCorp LP, College Station, TX).

3. Results

Disc pressure increased significantly with increasing follower load magnitude (Figure 3, Table 1) in all conditions at both T4-T5 and T8-T9, but the increase did not vary with rib cage condition. Disc pressure at T4-T5 without follower load was not different in the Stiffened condition than Intact, but was lower with No Ribs than Intact. In fact, measured T4-T5 pressure without follower load and No Ribs was at or below the minimum measureable pressure of the system in all specimens, and was thus recorded as 0 kPa. Disc

Author Manuscript Author Manuscript Author Manuscript Author Manuscript

pressure at T8-T9 without follower load was not different from Intact under Stiffened or No Ribs conditions. The difference between T4-T5 and T8-T9 pressure increased with follower load, such that T4-T5 pressure was 103 kPa higher than T8-T9 at 400 N follower load ($p = 0.037$), and 139 kPa higher at 600 N follower load ($p = 0.005$).

Overall T1-T12 sagittal plane curvature angle (Figure 4, Table 2) with no follower load was higher (more kyphotic) in the Stiffened and in the No Ribs conditions than in the Intact condition. There was no effect of follower load on T1-T12 angle in any condition. Regionally, T1-T4 angle increased with follower load in all conditions, but there were no differences between conditions in T1-T4 angle with no follower load or in change of T1-T4 angle with follower load. The T4-T8 angle with no follower load was larger in the No Ribs condition than Intact, but there was no difference between Stiffened and Intact, and no effect of follower load on T4-T8 angle. The T8-T12 angle decreased (became less kyphotic) with increasing follower load in all conditions. Additionally, T8-T12 angle with no follower load was larger in the Stiffened condition than Intact, but there was no difference between No Ribs and Intact.

In individual levels, T1-T2 sagittal plane angle (Figure 5, Table 2) increased with follower load in all conditions and was larger in the No Ribs condition than Intact with no follower load. The T4-T5 and the T8-T9 sagittal plane angles did not vary between conditions or with follower load. The T11-T12 sagittal plane angle was initially negative (lordotic) on average, and decreased (became more lordotic) with increasing follower load in all conditions. However, the T11-T12 angle with no follower load was larger with No Ribs than Intact, becoming slightly kyphotic in that condition, but the decrease with follower load was larger with No Ribs than Intact.

4. Discussion

This study examined the effects of follower load and rib cage on intervertebral disc pressures and sagittal plane thoracic curvature in static, upright, unconstrained loading conditions. This is the first study to examine thoracic intervertebral disc pressures in tests of cadaveric full thoracic spines, but the pressures measured here and trends with follower load compare well with previous reports. Disc pressure increased linearly with follower load (Figure 3), consistent with previous reports of increased lumbar disc pressure under follower load (Buttermann and Beaubien, 2008; Rohlmann et al., 2001; Wilke et al., 2003). In particular, Buttermann and Beaubien (2008) reported linear increases in L4-L5 disc pressures under follower loads from 0 to 1500 N, with a slope of pressure with increase with follower load if about 0.8 kPa/N, lower than the 1.00 kPa/N at T8-T9 and 1.24 kPa/N at T4-T5 in the current study. It is likely that the sensitivity of disc pressure to compressive loading is higher in more proximal levels of the spine, perhaps due to smaller cross-sectional area of the disc at superior levels of the spine, an idea which is also supported by the data of Dolan et al. (2013). In a more direct comparison, an average pressure of 1,270 kPa was reported for T8-T9 motion segments under a direct compressive load of 1,000 N (Dolan et al., 2013). The regression for Intact T8-T9 pressure (Table 1) predicts an average T8-T9 pressure of 1,089 kPa (95% confidence interval 875 – 1,304 kPa) at a follower load of 1,000 N, encompassing

Author Manuscript Author Manuscript Author Manuscript Author Manuscript

the previously reported value for directly applied compressive loads. This indicates that the follower load primarily applies compression across each intervertebral joint.

Comparing disc pressures from the current study with *in vivo* reports provides a means to evaluate follower load magnitudes that should be employed to simulate physiologically realistic compressive loading in the thoracic spine. Previous *in vivo* measurements of thoracic disc pressures have been reported for a variety of activities (Polga et al., 2004), for example with pressures during upright standing of 1,010±60 kPa for mid-thoracic discs (primarily T6-T7), and 860±60 kPa for lower thoracic discs (primarily T9-T10). However, the *in vivo* pressure measures of Polga et al. (2004) are not directly comparable with the current *in vitro* measurements for several reasons. In addition to measuring at different levels than the current study, there may be differences between *in vivo* and *in vitro* disc pressures that are not fully understood. For example prolonged compressive loading during *in vitro* testing can decrease fluid in intervertebral discs (McMillan et al., 1996) as well disc pressure (Adams et al., 1996a), although this may also happen *in vivo* as discs lose volume during daily loading (Botsford et al., 1994). Perhaps more importantly, disc degeneration reduces measured disc pressure (Buttermann and Beaubien, 2008), but discs were not graded in the current study. The subjects tested *in vivo* by Polga et al. (Polga et al., 2004) were young, with a mean age of 28 years, and measures were collected only on healthy discs, while some of the specimens in the current study, with a mean age of 67, almost certainly had disc degeneration present, as the prevalence of thoracic disc degeneration is more than 60% in individuals over the age of 60 (Teraguchi et al., 2014). Adams et al (1996b) report a 30% decline in nucleus pressure in lumbar discs over a similar age span *in vitro*, primarily the result of disc degeneration. Despite these differences, *in vivo* thoracic disc pressures may still provide useful guidance for the use of follower loads. For example, assuming a 30% reduction due to age-related degeneration, the study of Polga et al. (2004) suggests pressures of 707 kPa for mid-thoracic discs and 602 kPa for lower thoracic discs during upright standing in older adults. Based on the current results, pressures of 707 kPa at T4-T5 and 602 kPa at T8-T9 would require follower loads of about 425 N and 508 N, respectively, in the Intact condition. Recent musculoskeletal modeling estimates of thoracic loading in upright standing show a range from about 175 N at T1 to about 475 N at T12 (Bruno et al., 2015). Taken together, these values suggest that reasonable follower load magnitudes to simulate upright standing range from about 200 N in the upper thoracic spine to about 500 N in the lower thoracic spine. Since the follower load technique presented here applies the same load across the whole length of the spine, a load of about 400 N is a reasonable single magnitude load to simulate upright standing. Reasonable follower load levels for other activities or loading conditions may be estimated in a similar manner. It should be noted that the follower load technique presented applies a similar amount of compression at all levels of the spine and is not normalized to the specimen size. This is likely the reason for higher pressures at T4-T5 than T8-T9, with similar loading applied to both discs even though the T4-T5 disc is smaller.

The effect of rib cage condition on disc pressure was limited to T4-T5 where the No Ribs condition showed reduced pressure. This was counter to our hypothesis, as it suggests reduced compressive loading with the rib cage removed. However, given that the No Ribs condition was necessarily the last one tested, it is also possible that testing order was

Author Manuscript Author Manuscript Author Manuscript Author Manuscript

responsible for this difference. While the specimens were kept moist throughout testing, prolonged compressive loading is known to cause loss of fluid from intervertebral discs (McMillan et al., 1996) and a decrease in nucleus pressure (Adams et al., 1996a) in *in vitro* spine tests. An examination of pressure measurements performed throughout the testing process (data not shown) indicates a significant decline in pressure during the testing period at T4-T5 ($p < 0.001$), but not at T8-T9 ($p = 0.759$). Thus, evidence regarding the effect of rib cage condition may be confounded by the testing order. While the order of testing was a necessary limitation of this type of cadaveric study, in this case it limits the conclusions that can be drawn. This analysis was also limited to pressures in an unconstrained static upright position, and it is likely that the results are not representative of disc pressures under dynamic conditions, which will be reported in future analyses.

The overall sagittal plane curvature was not affected by follower load, which shows that the follower load application with the rib cage intact was successful in applying a compressive load without inducing changes in sagittal plane alignment. In applying a follower load to the thoracic spine without rib cage, Stanley et al. (2004) optimized the follower load by adjusting the location of the cable to minimize overall changes in curvature with increasing follower load magnitude. The reported average change in T2-L1 kyphosis was 2.3 ± 1.6° under an optimized 800 N follower load, not significantly different than the average change in No Ribs T1-T12 kyphosis of 3.0 ± 4.2° under 600 N follower load in the current study. Thus, while no follower load optimization was performed, the follower load in this study produced similar average changes in curvature. However, the changes in regional and level-specific curvatures with follower load may be the result of the lack of an optimization step. Specifically, the superior end of the spine became more flexed with increasing follower load, while the inferior end became less flexed or more extended. This suggests the follower load attachments were positioned anterior to optimal in the superior spine, but posterior to optimal in the inferior spine. While the follower load attachments were fixed in place due to the challenge of implementing the follower load inside the rib cage, this limitation could be addressed in future studies.

The overall curvature of the spine increased in both Stiffened and No Ribs conditions. The Stiffened rib cage increased flexion primarily in the lower thoracic spine region, neared significance in the upper spine (T1-T4, $p = 0.071$), but caused no change in the T4-T8 region. Interestingly, the upper and middle regions with little or no change overlap with the plates applied at ribs 2 – 5. The stiffened rib cage condition does not directly represent a realistic *in vivo* condition, although it is possible that age-related increases in costal cartilage calcification (Teale et al., 1989) or sternocostal joint osteophytes (Schils et al., 1989) could act to locally stiffen the rib cage in this manner. Nonetheless, the effects demonstrate that alterations in rib cage mechanics can significantly alter the baseline curvature of the thoracic spine. The No Ribs condition increased flexion throughout the spine, including upper (T1-T2 angle), middle region (T4-T8) and lower (T11-T12). The lower spine, and specifically T11-T12 angle, showed a larger change in angle with follower load with No Ribs than Intact, suggesting that the rib cage provided support even to this level of the spine. Overall, the increased flexion seen with No Ribs suggests that the rib cage helped support the spine before it was removed. This could be due in part to the forward leaning orientation of the

Author Manuscript Author Manuscript Author Manuscript Author Manuscript

spines during testing (see Figure 2), where the loss of rib cage support could allow the superior end of the specimen to fall forward and increase flexion.

In conclusion, a compressive follower preload was successfully applied to a full cadaveric thoracic spine with the rib cage intact. Intervertebral disc pressures were measured in the thoracic spine under follower load, and found to increase linearly with follower load magnitude, similar to lumbar disc pressures, although the effect of the rib cage on disc pressures in static conditions remains unclear. Follower load had no effect on sagittal plane spine curvature overall, despite the lack of an optimizing step, but produced more flexion in the upper spine, and less flexion in the lower spine. Rib cage stiffening and removal both increased overall spine flexion slightly, although with differing regional effects. The combination of follower load techniques and intact rib cage, as well as the measurement of thoracic disc pressures, add to the clinical relevance of *in vitro* studies of thoracic spine biomechanics, surgical procedures, and implant testing. This study provides a baseline to support such studies in the future.

Acknowledgments

This study was supported by the National Institute on Aging (K99AG042458) and by a Mentored Career Development Award from the American Society for Bone and Mineral Research. The study sponsors had no role in the study design, data collection, analysis, manuscript preparation, or the decision to submit the manuscript for publication.

References

Adams MA, McMillan DW, Green TP, Dolan P. Sustained loading generates stress concentrations in lumbar intervertebral discs. Spine. 1996a; 21:434–438. [PubMed: 8658246]

Adams MA, McNally DS, Dolan P. ‘Stress’ distributions inside intervertebral discs. The effects of age and degeneration. J Bone Joint Surg Br. 1996b; 78:965–972. [PubMed: 8951017]

Asher MA, Burton DC. Adolescent idiopathic scoliosis: natural history and long term treatment effects. Scoliosis. 2006; 1:2. [PubMed: 16759428]

Auerbach JD, Lonner BS, Errico TJ, Freeman A, Goerke D, Beaubien BP. Quantification of intradiscal pressures below thoracolumbar spinal fusion constructs: is there evidence to support “saving a level”? Spine. 2012; 37:359–366. [PubMed: 21540780]

Botsford DJ, Esses SI, Ogilvie-Harris DJ. In vivo diurnal variation in intervertebral disc volume and morphology. Spine. 1994; 19:935–940. [PubMed: 8009352]

Brasiliense LB, Lazaro BC, Reyes PM, Dogan S, Theodore N, Crawford NR. Biomechanical contribution of the rib cage to thoracic stability. Spine. 2011; 36:E1686–1693. [PubMed: 22138782]

Briggs AM, Bragge P, Smith AJ, Govil D, Straker LM. Prevalence and associated factors for thoracic spine pain in the adult working population: a literature review. J Occup Health. 2009; 51:177–192. [PubMed: 19336970]

Bruno AG, Bouxsein ML, Anderson DE. Development and Validation of a Musculoskeletal Model of the Fully Articulated Thoracolumbar Spine and Rib Cage. J Biomech Eng. 2015; 137:081003. [PubMed: 25901907]

Buttermann GR, Beaubien BP. In vitro disc pressure profiles below scoliosis fusion constructs. Spine. 2008; 33:2134–2142. [PubMed: 18794754]

Campbell RM Jr. VEPTR: past experience and the future of VEPTR principles. Eur Spine J. 2013; 22(Suppl 2):S106–117. [PubMed: 23354777]

Dolan P, Luo J, Pollintine P, Landham PR, Stefanakis M, Adams MA. Intervertebral disc decompression following endplate damage: implications for disc degeneration depend on spinal level and age. Spine. 2013; 38:1473–1481. [PubMed: 23486408]

Author Manuscript Author Manuscript Author Manuscript Author Manuscript

Healy AT, Mageswaran P, Lubelski D, Rosenbaum BP, Matheus V, Benzel EC, Mroz TE. Thoracic range of motion, stability, and correlation to imaging-determined degeneration. J Neurosurg Spine. 2015; 23:170–177. [PubMed: 25978074]

Kado DM, Prenovost K, Crandall C. Narrative review: hyperkyphosis in older persons. Annals of internal medicine. 2007; 147:330–338. [PubMed: 17785488]

Mannen EM, Anderson JT, Arnold PM, Friis EA. Mechanical analysis of the human cadaveric thoracic spine with intact rib cage. Journal of biomechanics. 2015a; 48:2060–2066. [PubMed: 25912664]

Mannen EM, Anderson JT, Arnold PM, Friis EA. Mechanical Contribution of the Rib Cage in the Human Cadaveric Thoracic Spine. Spine. 2015b; 40:E760–766. [PubMed: 25768687]

McMillan DW, Garbutt G, Adams MA. Effect of sustained loading on the water content of intervertebral discs: implications for disc metabolism. Ann Rheum Dis. 1996; 55:880–887. [PubMed: 9014581]

Nachemson A. Lumbar intradiscal pressure. Experimental studies on post-mortem material. Acta Orthop Scand Suppl. 1960; 43:1–104. [PubMed: 14425680]

Nachemson A, Morris JM. In Vivo Measurements of Intradiscal Pressure. Discometry, a Method for the Determination of Pressure in the Lower Lumbar Discs. J Bone Joint Surg Am. 1964; 46:1077–1092. [PubMed: 14193834]

Patwardhan AG, Havey RM, Meade KP, Lee B, Dunlap B. A follower load increases the load-carrying capacity of the lumbar spine in compression. Spine. 1999; 24:1003–1009. [PubMed: 10332793]

Perry TG, Mageswaran P, Colbrunn RW, Bonner TF, Francis T, McLain RF. Biomechanical evaluation of a simulated T-9 burst fracture of the thoracic spine with an intact rib cage. J Neurosurg Spine. 2014; 21:481–488. [PubMed: 24949903]

Polga DJ, Beaubien BP, Kallemeier PM, Schellhas KP, Lew WD, Buttermann GR, Wood KB. Measurement of in vivo intradiscal pressure in healthy thoracic intervertebral discs. Spine. 2004; 29:1320–1324. [PubMed: 15187632]

Pollintine P, Przybyla AS, Dolan P, Adams MA. Neural arch load-bearing in old and degenerated spines. Journal of biomechanics. 2004; 37:197–204. [PubMed: 14706322]

Rohlmann A, Neller S, Claes L, Bergmann G, Wilke HJ. Influence of a follower load on intradiscal pressure and intersegmental rotation of the lumbar spine. Spine. 2001; 26:E557–561. [PubMed: 11740371]

Sato K, Kikuchi S, Yonezawa T. In vivo intradiscal pressure measurement in healthy individuals and in patients with ongoing back problems. Spine. 1999; 24:2468–2474. [PubMed: 10626309]

Schils JP, Resnick D, Haghighi P, Trudell D, Sartoris DJ. Sternocostal joints. Anatomic, radiographic and pathologic features in adult cadavers. Invest Radiol. 1989; 24:596–603. [PubMed: 2777528]

Schultz A, Andersson G, Ortengren R, Haderspeck K, Nachemson A. Loads on the lumbar spine. Validation of a biomechanical analysis by measurements of intradiscal pressures and myoelectric signals. J Bone Joint Surg Am. 1982; 64:713–720. [PubMed: 7085696]

Stanley SK, Ghanayem AJ, Voronov LI, Havey RM, Paxinos O, Carandang G, Zindrick MR, Patwardhan AG. Flexion-extension response of the thoracolumbar spine under compressive follower preload. Spine. 2004; 29:E510–514. [PubMed: 15543052]

Teale C, Romaniuk C, Mulley G. Calcification on chest radiographs: the association with age. Age Ageing. 1989; 18:333–336. [PubMed: 2603842]

Teraguchi M, Yoshimura N, Hashizume H, Muraki S, Yamada H, Minamide A, Oka H, Ishimoto Y, Nagata K, Kagotani R, Takiguchi N, Akune T, Kawaguchi H, Nakamura K, Yoshida M. Prevalence and distribution of intervertebral disc degeneration over the entire spine in a population-based cohort: the Wakayama Spine Study. Osteoarthritis Cartilage. 2014; 22:104–110. [PubMed: 24239943]

Van der Klift M, De Laet CE, McCloskey EV, Hofman A, Pols HA. The incidence of vertebral fractures in men and women: the Rotterdam Study. J Bone Miner Res. 2002; 17:1051–1056. [PubMed: 12054160]

Watkins, Rt; Watkins, R., 3rd; Williams, L.; Ahlbrand, S.; Garcia, R.; Karamanian, A.; Sharp, L.; Vo, C.; Hedman, T. Stability provided by the sternum and rib cage in the thoracic spine. Spine. 2005; 30:1283–1286. [PubMed: 15928553]

Author Manuscript Author Manuscript Author Manuscript Author Manuscript

Wilke H, Neef P, Hinz B, Seidel H, Claes L. Intradiscal pressure together with anthropometric data--a data set for the validation of models. Clinical biomechanics (Bristol, Avon). 2001; 16(Suppl 1):S111–126.

Wilke HJ, Rohlmann A, Neller S, Graichen F, Claes L, Bergmann G. ISSLS prize winner: A novel approach to determine trunk muscle forces during flexion and extension: a comparison of data from an in vitro experiment and in vivo measurements. Spine. 2003; 28:2585–2593. [PubMed: 14652475]

Wilke HJ, Wenger K, Claes L. Testing criteria for spinal implants: recommendations for the standardization of in vitro stability testing of spinal implants. Eur Spine J. 1998; 7:148–154. [PubMed: 9629939]

Author Manuscript Author Manuscript Author Manuscript Author Manuscript

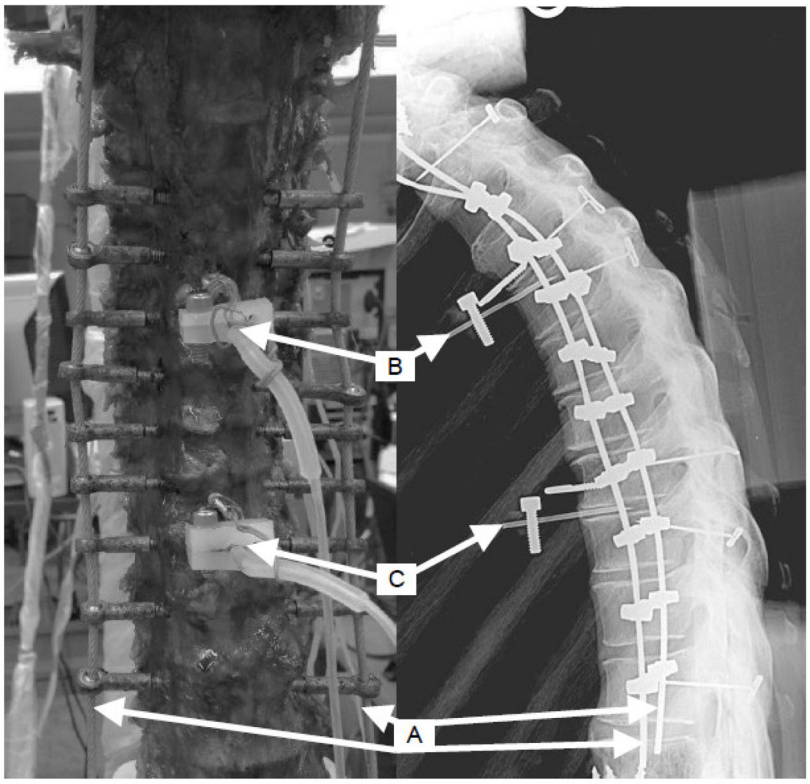

Figure 1.

Anterior view of a specimen with ribcage removed (left), and lateral x-ray view of a specimen with ribcage intact (right). Follower load application was via bilateral cables (A) attached to T1 and threaded through eye nuts attached to rods through vertebral bodies T3 – T11. Pressure transducer needles were inserted in the T4-T5 (B) and T8-T9 (C) intervertebral discs.

Author Manuscript Author Manuscript Author Manuscript Author Manuscript

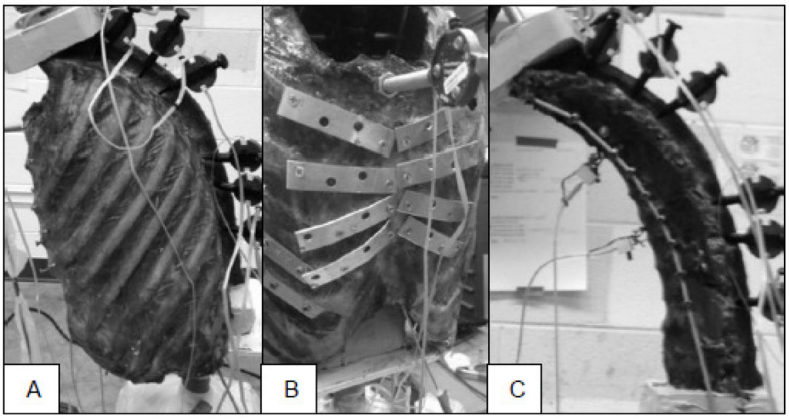

Figure 2.

Rib cage conditions included A) unaltered intact rib cage; B) stiffened rib cage; and C) rib cage removed. Each condition was tested under four follower loads (0, 200, 400 and 600 N).

Author Manuscript Author Manuscript Author Manuscript Author Manuscript

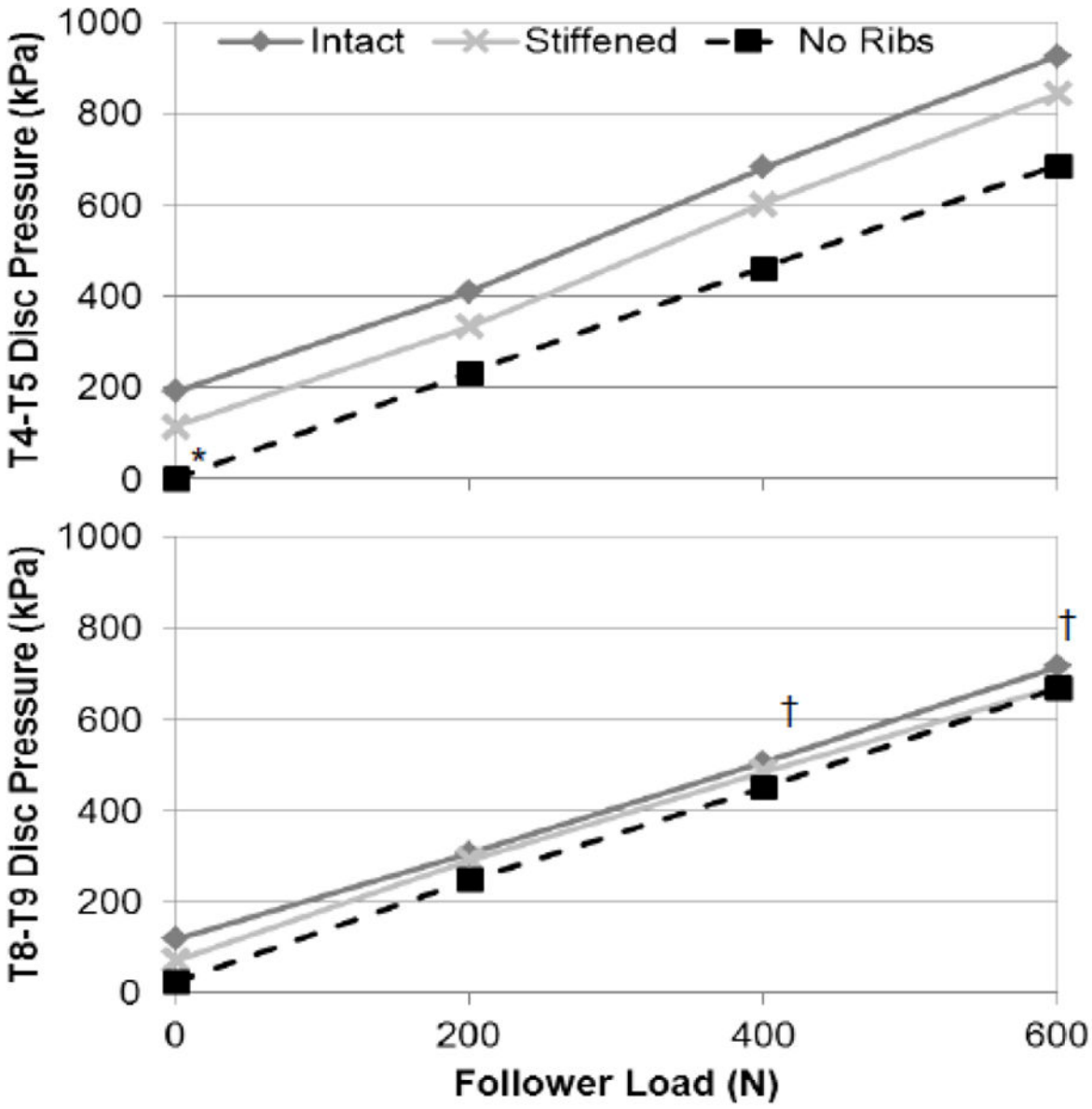

Figure 3.

Mean pressures in the T4-T5 (top) and T8-T9 (bottom) intervertebral discs under different testing conditions and follower loads. Pressures increased significantly with follower load in all cases ($p < 0.001$). *Pressure different at 0 follower load than Intact ($p < 0.05$); †Significant pressure difference between levels ($p < 0.05$).

Author Manuscript Author Manuscript Author Manuscript Author Manuscript

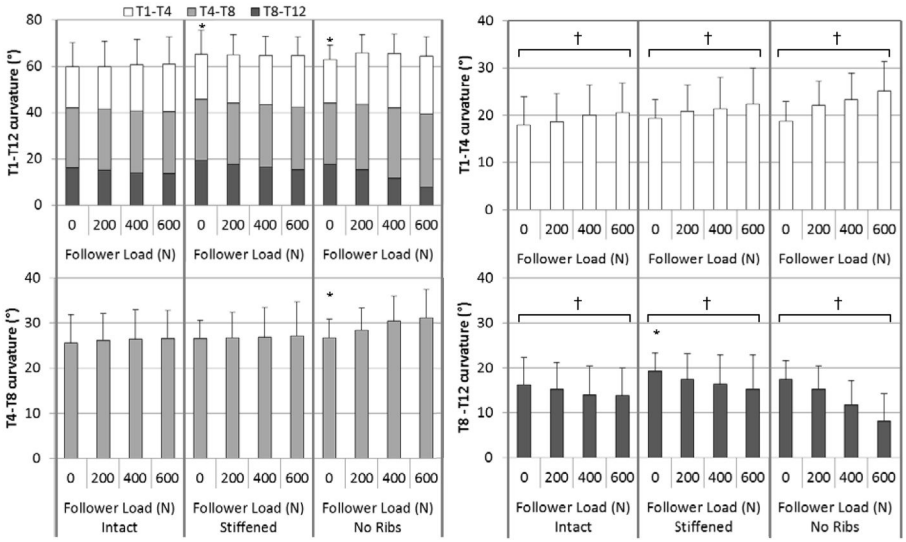

Figure 4.

Mean sagittal spine curvature overall (T1-T12, upper left), and regionally (T1-T4, upper right; T4-T8, lower left; and T8-T12, lower right) by follower load and rib cage conditions. Error bars indicate one standard deviation. *Curvature at 0 N follower load different than Intact ($p < 0.05$); †Significant angle change with follower load ($p < 0.05$).

Author Manuscript Author Manuscript Author Manuscript Author Manuscript

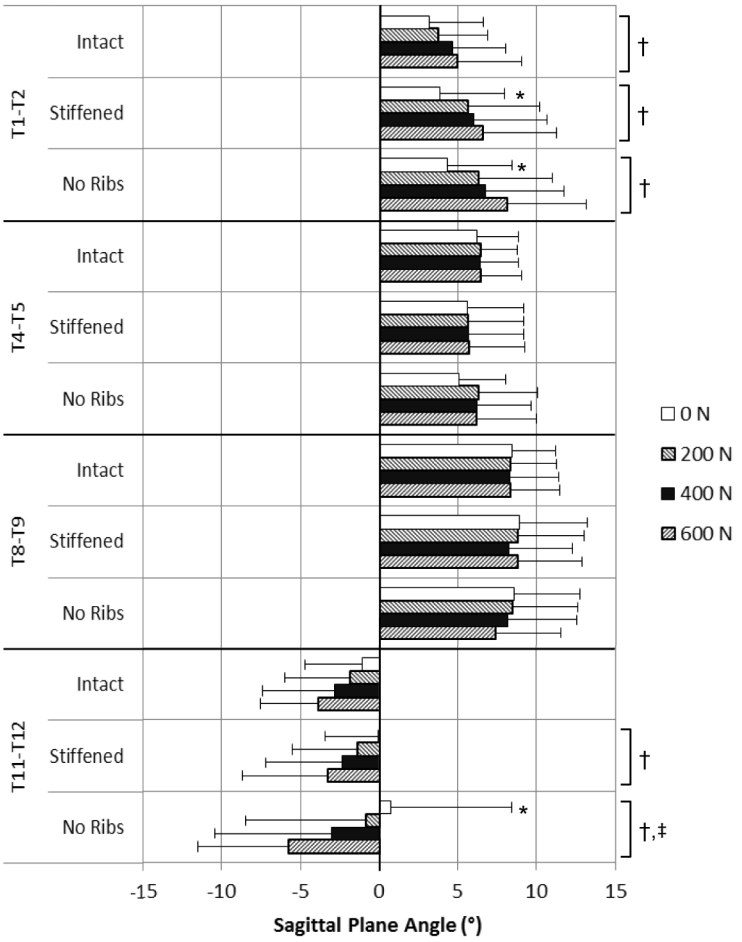

Figure 5.

Mean sagittal plane angles at individual levels by follower load and rib cage condition. Positive indicates a flexed (kyphotic) position, while negative indicates an extended (lordotic) position. Error bars indicate one SD in the direction of the mean. *Angle different in stiffened or no ribs condition than intact ($p < 0.05$); †Significant angle change with follower load ($p < 0.05$); ‡Change with follower load different than Intact ($p < 0.05$).

Author Manuscript Author Manuscript Author Manuscript Author Manuscript

Table 1

Estimates (95% confidence intervals) of regression coefficients for the effect of follower load on disc pressure by test condition. P-values are shown for difference of estimates from the Intact condition and for significance of slope (change with follower load).

	Constant (kPa)	Slope (kPa/N)	p-values		
			Constant vs. Intact	Slope vs. Intact	Slope vs. 0
T4-T5 Pressure					
Intact	180 (26 – 333)	1.24 (1.04 – 1.44)	-	-	< 0.001
Stiffened	99 (−57 – 256)	1.23 (1.02 – 1.44)	0.148	0.943	< 0.001
No Ribs	−3 (−159 – 154)	1.14 (0.93 – 1.35)	0.001	0.514	< 0.001
T8-T9 Pressure					
Intact	94 (−65 – 253)	1.00 (0.77 – 1.22)	-	-	< 0.001
Stiffened	82 (−73 – 236)	1.00 (0.79 – 1.21)	0.834	0.986	< 0.001
No Ribs	29 (−126 – 184)	1.07 (0.86 – 1.28)	0.277	0.652	< 0.001

Author Manuscript Author Manuscript Author Manuscript Author Manuscript

J Biomech. Author manuscript; available in PMC 2017 May 03.

Table 2

Estimates (95% confidence intervals) of regression coefficients for the effect of follower load on overall, regional, and individual level sagittal plane angles by test condition. P-values are shown for difference of estimates from the Intact condition and for significance of slope (change with follower load).

	Constant (°)	Slope (°/kN)	p-values		
			Constant vs. Intact	Slope vs. Intact	Slope vs. 0
Overall (T1-T12) angle					
Intact	59.7 (52.9 – 66.4)	2.20 (−1.84 – 6.24)	-	-	0.285
Stiffened	65.1 (58.4 – 71.8)	−0.80 (−4.84 – 3.23)	< 0.001	0.302	0.696
No Ribs	63.9 (57.1 – 70.7)	4.16 (−0.51 – 8.83)	< 0.001	0.534	0.081
Regional angles T1-T4 angle					
Intact	17.8 (13.9 – 21.8)	4.77 (1.36 – 8.19)	-	-	0.006
Stiffened	19.5 (15.6 – 23.4)	4.84 (1.43 – 8.25)	0.071	0.979	0.005
No Ribs	19.1 (15.1 – 23.1)	9.54 (5.59 – 13.48)	0.205	0.074	< 0.001
T4-T8 angle					
Intact	25.8 (20.8 – 30.7)	1.56 (−1.81 – 4.92)	-	-	0.364
Stiffened	26.6 (21.6 – 31.5)	0.89 (−2.48 – 4.25)	0.386	0.783	0.605
No Ribs	27.8 (22.8 – 32.8)	2.94 (−0.95 – 6.84)	0.035	0.598	0.139
T8-T12 angle					
Intact	16.1 (9.0 – 23.1)	−4.13 (−7.60 – −0.67)	-	-	0.019
Stiffened	19.0 (12.0 – 26.1)	−6.53 (−10.00 – −3.07)	0.001	0.337	< 0.001
No Ribs	17.1 (10.1 – 24.2)	−8.74 (−12.49 – −5.00)	0.262	0.076	< 0.001
Individual Angles T1-T2 angle					
Intact	3.17 (0.37 – 5.96)	3.18 (0.71 – 5.65)	-	-	0.012
Stiffened	4.35 (1.54 – 7.16)	3.97 (1.41 – 6.52)	0.084	0.664	0.002
No Ribs	4.68 (1.85 – 7.50)	5.88 (3.13 – 8.63)	0.03	0.152	< 0.001
T4-T5 angle					
Intact	6.29 (4.18 – 8.40)	0.34 (−2.00 – 2.68)	-	-	0.777
Stiffened	5.56 (3.45 – 7.67)	0.19 (−2.15 – 2.52)	0.252	0.928	0.876

Author Manuscript Author Manuscript Author Manuscript Author Manuscript

	Constant (°)	Slope (°/kN)	p-values		
			Constant vs. Intact	Slope vs. Intact	Slope vs. 0
No Ribs	5.93 (3.76 – 8.11)	1.02 (−1.70 – 3.74)	0.606	0.709	0.461
T8-T9 angle					
Intact	8.37 (5.85 – 10.90)	−0.20 (−3.05 – 2.64)	-	-	0.888
Stiffened	8.87 (6.34 – 11.40)	−0.18 (−3.04 – 2.67)	0.516	0.992	0.9
No Ribs	8.59 (6.06 – 11.12)	−0.86 (−3.93 – 2.21)	0.776	0.759	0.584
T11-T12 angle					
Intact	−1.25 (−4.94 – 2.43)	−2.92 (−6.28 – 0.44)	-	-	0.089
Stiffened	−0.17 (−3.85 – 3.52)	−5.35 (−8.60 – −2.10)	0.218	0.308	0.001
No Ribs	0.77 (−2.92 – 4.46)	−8.15 (−11.81 – −4.48)	0.023	0.039	< 0.001